Available online at www.sciencedirect.com
ScienceDirect
Journal of the European Ceramic Society 30 (2010) 283–287
www.elsevier.com/locate/jeurceramsoc

Growth and characterisation of multiferroic $BiFeO_3$ films with fully saturated ferroelectric hysteresis loops and large remanent polarisations

Xiaoding Qi [a,*], Wen-Chih Chang [a], Jui-Chao Kuo [a], In-Gann Chen [a], Yi-Chun Chen [b], Cheng-Hung Ko [b], Jung-Chun-Andrew Huang [b]

[a] *Department of Materials Science and Engineering, National Cheng Kung University, Tainan City 701, Taiwan*
[b] *Department of Physics, National Cheng Kung University, Tainan City 701, Taiwan*

Available online 21 June 2009

Abstract

Multiferroic $BiFeO_3$ films have been deposited on a number of substrates by RF magnetron sputtering. Two routes were adopted in order to obtain the films of high phase purity and accurate stoichiometry. The first was to sputter films at room temperature and then the $BiFeO_3$ phase was formed after sintering at various temperatures under controlled ambient atmosphere. The second was to grow $BiFeO_3$ in-situ at high temperature during sputtering. Although the sintered films grown on $SrTiO_3$ substrates were epitaxial and showed better texture than the in-situ films, they had much poorer ferroelectric properties, due to the residual traces of intermediate phases formed during heating. Under right growth parameters, the in-situ films grown on the $LaNiO_{3-x}$ buffered $SrTiO_3$ showed fully saturated ferroelectric hysteresis loops with large remanent polarisation of 64 $\mu C/cm^2$. Piezoresponse force microscopy (PFM) was used to examine the ferroelectric domain structures. When scanned without DC bias, fine spontaneous domains were observed. Under ± 10 V DC bias, PFM confirmed that the domains could be poled and switched.

Keywords: Multiferroic; $BiFeO_3$; Magnetron sputtering; Thin film

1. Introduction

Significant advances in both thin film growth and characterisation techniques during the past 20 years or so have recently brought about a renewed interest in the magnetoelectric multiferroics,[1–4] which are simultaneously ferroelectric and (anti-)ferromagnetic. In addition to the importance in the understanding of fundamental physics, the coexistence of ferroelectric and magnetic domains in a single material provides a brand-new platform for the designing of next-generation devices beyond the reach of currently available materials. As far as the device applications concerned, $BiFeO_3$ (BFO) is no doubt one of the best choices, because both its ferroelectric and magnetic transition points are well above room temperature (i.e. ferroelectric $T_c = 770\,^{\circ}C$ and antiferromagnetic $T_N = 374\,^{\circ}C$[5,6]). However, high-quality BFO samples with good ferroelectric properties have been extremely difficult to grow. Bulk single crystals often showed a small remanent polarisation of about 3.5 $\mu C/cm^2$[2,7] which is inconsistent with its high T_c. A much higher remanence (>50 $\mu C/cm^2$) was first demonstrated in the thin film samples and the great improvement was attributed to the heteroepitaxy-induced structural distortions.[8] However, recent advance in the growth technique has made higher-quality single crystals available, which also showed a same magnitude of remanence.[9] Therefore large remanent polarisation is intrinsic to BFO, but often poor quality of the samples has prevented it from achieving such a value. More researches on the film growth are required in order to optimise ferroelectric properties and to improve the reproducibility of good samples.

2. Experimental method

In this study, the films were grown by RF magnetron sputtering. BFO targets of 2-in. diameter were prepared by sintering the 1.02:1 mixtures of Bi_2O_3 (99.9 at.%) and Fe_2O_3 (99.9 at.%) in air at 800 °C. The small excess of Bi_2O_3 was intended to compensate the preferential loss of bismuth during sintering. The target was checked by X-ray diffraction (XRD) to be BFO with small amount of $Bi_{25}FeO_{40}$ [10] and $Bi_2Fe_4O_9$.[11] However, energy dispersive X-ray spectroscopy (EDXS) showed that the overall composition had the Bi:Fe ratio equal to 1 within the

* Corresponding author. Tel.: +886 6 2008060; fax: +886 6 2346290.
E-mail address: xqi045@mail.ncku.edu.tw (X. Qi).

0955-2219/$ – see front matter © 2009 Elsevier Ltd. All rights reserved.
doi:10.1016/j.jeurceramsoc.2009.05.038

experimental error. BFO Films were grown on the Si, $LaAlO_3$ (LAO), $SrTiO_3$ (STO), and $LaNiO_{3-x}$ (LNO) buffered STO substrates. The conductive LNO layer, which was used as the bottom electrode for ferroelectric measurements, was sputtered on STO by the same system at the temperature of 650 °C and the oxygen partial pressure (pO_2) of 10 mTorr. LNO targets were prepared by sintering the 2:1 mixtures of NiO and La_2O_3 at 1300 °C in air. XRD showed that LNO films were epitaxially grown on STO and had a very similar pattern to a known phase.[12] Atomic force microscopy (AFM) showed typical root-mean-square (rms) roughness of about 1.0 nm for the LNO films of thickness 30–50 nm and 10 nm for the films of thickness over 100 nm. The conductivity of LNO films was measured to be in the order of $10^3\ \Omega^{-1}\ cm^{-1}$.

Initially, several batch of BFO films were deposited at room temperature and then taken out from the sputtering chamber and annealed in the tube furnaces at temperatures between 400 and 700 °C in various ambient atmospheres, including air and flowing O_2, Ar and Ar + 3%H_2, respectively. This was intended to quickly find suitable thermodynamic parameters for the growth of pure BFO films. The films were deposited with the following sputtering parameters: power 100 W, background vacuum 5×10^{-6} Torr, and working Ar pressure 30–50 mTorr with flow rate of 30 sccm. At a later stage, the films were grown at high temperatures to form the BFO phase in-situ during sputtering. In this case, the pO_2 and the substrate temperature inside the sputtering chamber were the thermodynamic parameters used to control the impurity phases present in the films, while the sputtering rate was fixed at a relatively high value of about 5 nm/min. Based on the earlier annealing results, the substrate temperatures were tried between 550 and 650 °C and a relatively low pO_2 of 20 mTorr or below were used.

The prepared films were studied by a range of characterisation methods. Rigaku MultiFlex XRD diffractometer was used for wide-range θ–2θ scans. Glancing-incident-angle (2°) XRD (GIAXRD) and the high-resolution ω and φ scans were recorded with a Rigaku ATX-E diffractometer. AFM and PFM were performed by the Digital Instruments CP-II system, Veeco Instruments Inc. Ferroelectric measurements were carried out by the Precision Ferroelectric Tester, Radiant Technologies Inc. The top electrode was Pt, which was evaporated with a mask of holes of 200-μm diameter. The bottom electrode was epitaxial LNO (∼50 nm thick) as described above.

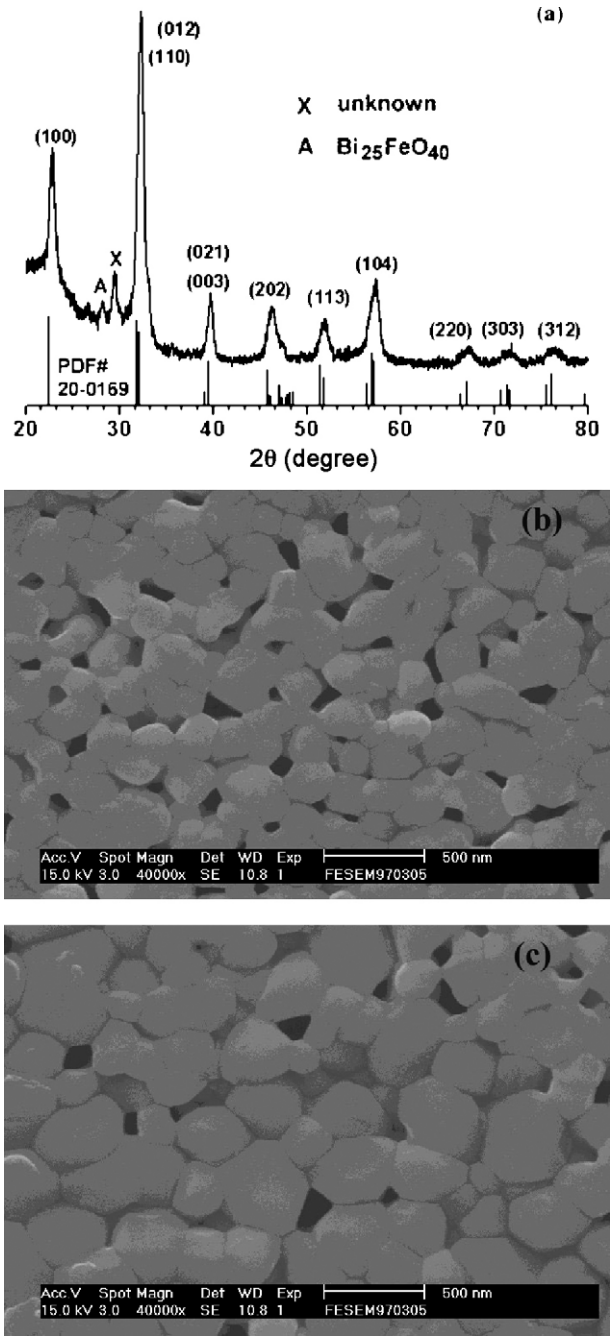

Fig. 1. (a) GIAXRD of the film deposited on Si at room temperature and annealed at 600 °C in Ar for 1 h. (b and c) SEM images for films sintered at 650 °C in Ar for 10 min and 2 h, respectively.

3. Results

3.1. Films deposited at room temperature

It was found that the minimum temperature for the formation of the BFO phase was about 550 °C, below which no clear set of reflection lines for the BFO phase could be identified in XRD after prolonged sintering for 12 h. However, higher crystallinity was achieved at 600 °C, which was indicated by the intense and sharp XRD lines, as shown in Fig. 1a. $Bi_{25}FeO_{40}$ and another unknown phase with a marked reflection at $2\theta = 29.3°$ were also present in the films. At higher sintering temperatures, e.g. 700 °C, $Bi_{25}FeO_{40}$ disappeared completely, but the amount of the unknown phase also increased. When the Si substrates were used, it was unable to get rid of the unknown phase completely after many attempts by sintering in different ambient atmospheres described above, although we did find that the films sintered in Ar contained the least amount of impurity. Well defined BFO grains could be formed after 10 min sintering at 650 °C in Ar, as shown in the scanning electron microscopy (SEM) in Fig. 1b. Prolonged sintering time of 2 h only resulted in moderate increase in film density and grain size (Fig. 1c).

When (0 0 1) STO substrates were used, pure BFO could be formed by sintering at 650 °C in Ar for 1 h, as showed in the

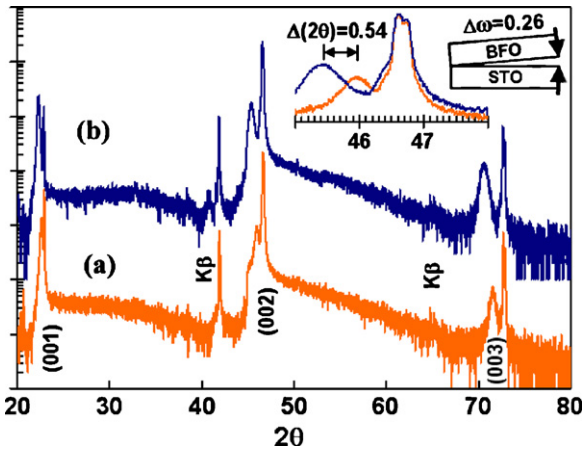

Fig. 2. XRD θ–2θ scans of the films (a) sintered, (b) sputtered in-situ. *Inset*: enlargement of (0 0 2) reflections, showing 2θ shift of 0.54°. *Top right corner*: tilting of BFO revealed by the ω scans.

XRD θ–2θ scans (Fig. 2a), which recorded only the (0 0 l) (l = 1, 2, 3) reflections of BFO and STO, indicating that the film were c-textured and pure (note: the intensity in Fig. 2 was plotted in logarithmic scale to magnify weak reflection). Although pure BFO could also be formed by sintering in air, mixed textures were obtained. High-resolution XRD ω-scans were carried out to determine the out-of-plane texture of the films grown on (0 0 1) STO and the full width at half maximum (FWHM) of the (0 0 2) reflection was measured to be 1.0° (inset of Fig. 3). XRD φ-scan confirmed that the films were also in-planed aligned with FWHM = 1.7°, as shown in Fig. 3. Epitaxial BFO films could also be grown on the (0 0 1) LAO substrates by sintering at 650 °C in Ar, however there was a weak peak unidentified in XRD, as shown in Fig. 4a. With the sputtering parameters given in the experiment section, the deposition rate was measured to be about 4.5 nm/min. One-hour deposition time typically gave a film thickness of about 270–300 nm after sintering. The dependence of film thickness and surface roughness (after sintering) as a function of the deposition time is shown in Fig. 5.

3.2. Films deposited at high temperature

The experiment results showed that the phases present in the films were also dependent on the substrates used. For the STO substrates, which had a lattice misfit of 1.3%, pure BFO

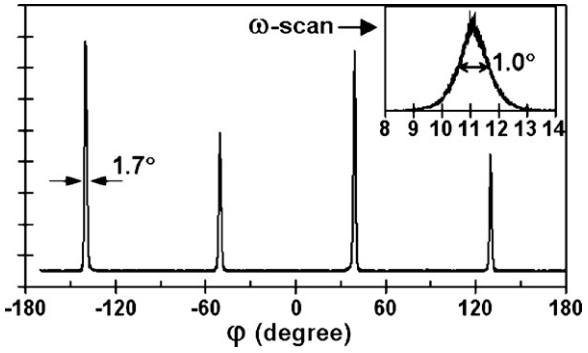

Fig. 3. φ-Scan of sintered films. *Inset*: ω-scan.

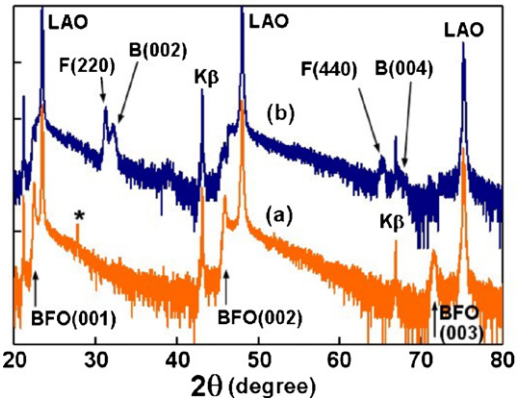

Fig. 4. XRD θ–2θ scans of films on (0 0 1) LAO. (a) Sintered at 650 °C in flowing Ar for 40 min. (b) Grown in-situ at 600 °C, 5 mTorr pO_2. Sputtering time: 1 h; power: 100 W; F = Fe_3O_4; B = $Bi_{3.43}Fe_{0.57}O_6$; *: unknown.

Table 1
Impurity phases present in the films grown on (0 0 1) LAO at 600–650 °C.

pO_2 (mTorr)	≤1	>1	≥17
Impurity phases	Fe_3O_4	Fe_3O_4 + $Bi_{3.43}Fe_{0.57}O_6$	$Bi_{3.43}Fe_{0.57}O_6$ + α-Fe_2O_3

films could be grown over a small window of conditions, however the optimum conditions for the ferroelectric properties were found to be pO_2 2 mTorr and substrate temperature 600 °C. The films grown on (0 0 1) STO were epitaxial with the out-of-plane and in-plane textures (FWHM) of 1.6° and 1.4°, respectively. A typical XRD θ–2θ scan is shown in Fig. 2b for comparison with the films formed by sintering. On the other hand, for the (0 0 1) LAO substrates, which had a larger misfit of 4.2%, the film growth was much more complicated as compared to that by sintering. XRD identified three impurity phases present in the films grown at 600–650 °C. Depending on the pO_2 during sputtering, the impurity phases could be Fe_3O_4,[13] $Bi_{3.43}Fe_{0.57}O_6$ [14] and α-Fe_2O_3,[15] as summarised in Table 1. The XRD pattern of a film sputtered at 600 °C and 5 mTorr pO_2 is shown in Fig. 4b for comparison. In this particular case the dominant phases in the film were actually Fe_3O_4 and $Bi_{3.43}Fe_{0.57}O_6$.

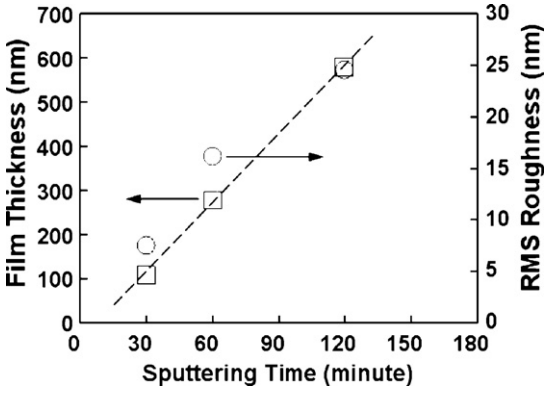

Fig. 5. Film thickness and surface roughness as the function of growth time (after sintered in Ar for 1 h).

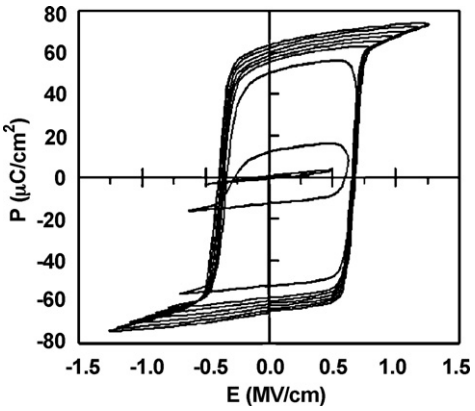

Fig. 6. *P–E* hysteresis loops of BFO films grown in-situ on (0 0 1) LNO/STO, measured at 27 °C.

4. Discussions

Although BFO films could be grown epitaxially on (0 0 1) STO either by sputtering at high temperature or by post-deposition annealing, the textures of the resultant films were different. As shown in Fig. 2, the out-of-plane texture for the BFO film formed in-situ was much larger, which had FWHM = 1.6° compared to 1.0° for the post-deposition annealed film. In contrast, the in-plane texture of the in-situ film was slightly smaller. An apparent shift of 2θ for the BFO films was observed, as highlighted in the inset of Fig. 2 for the (0 0 2) reflections. This was unlikely to be caused by the heteroepitaxy-induced structural distortions, because both films had a thickness of about 300 nm. With such a thickness, strains should have relaxed already.[16] The shift was found to arise from the slight tilt of BFO (0 0 1) plane against STO (0 0 1) plane, as illustrated in the inset of Fig. 2. This was confirmed by the high-resolution XRD ω-scans for the BFO (0 0 2) and the STO (0 0 2) reflections, respectively, which revealed that there was 0.26° difference between the two offset angles for the in-situ film. This matched very well with the θ–2θ scan, which showed a 2θ shift of 0.54° (i.e. $\Delta\theta = 0.27°$). The texture difference might result from the different dynamic process during the film growth in these two routes. There was a large supersaturation for the in-situ films sputtered around 600 °C and hence a much higher growth rate, compared to the films sintered after deposition. In the in-situ route, the large supersaturation also drove the growth of other phases that did not normally occur under the conditions close to equilibrium. This might account for the more impurity phases observed on the LAO substrates, whose large lattice misfit less favoured BFO growth. There was a large difference in the ferroelectric properties between the BFO films formed in-situ and post-deposition annealing. The post-deposition annealed films generally showed a very large leakage current, and the polarisation-electric field (*P–E*) hysteresis loops were unable to reach a saturated state, resulting in a very small remanent polarisation. One of the main causes for large leakage current in BFO has been attributed to the oxygen vacancies resulted from the nonstoichiometry of BFO,[17,18] which was related with preferential loss of Bi at high temperature due to much higher vapour pressure of the bismuth oxide than iron oxide.[19,20] It was thought that post-deposition annealing might give the films a better stoichiometry if the as-deposited composition at room temperature was accurate and the subsequent sintering time was short. Therefore a low leakage might be expected. However, the result turned up to be the opposite way. In order to identify the cause, high-resolution compositional analysis methods, such as X-ray photoemission spectroscopy (XPS), were used to check the film compositions. The result showed that the sintered films had the Bi/Fe ratio equal to 1.0082, extremely close to the stoichiometric composition. The cause for the high leakage current was more likely to arise from the residual traces of the intermediate impurity phases mentioned in the last section. Although XRD showed a pure BFO phase for the films sintered on STO, typical precision of XRD phase identification was only about 1%. Such an amount of impurity would be enough to cause a significant leakage. Because both Bi-rich and Fe-rich phases (e.g. $Bi_{25}FeO_{40}$ and $Bi_2Fe_4O_9$) were possibly present in the films, XPS would still tell a right composition in such a case.

Good ferroelectric properties were achieved for the films grown on STO at high temperature. The level of leakage was much lower compared to those films formed by sintering, presumably due to the higher phase purity as well as an accurate

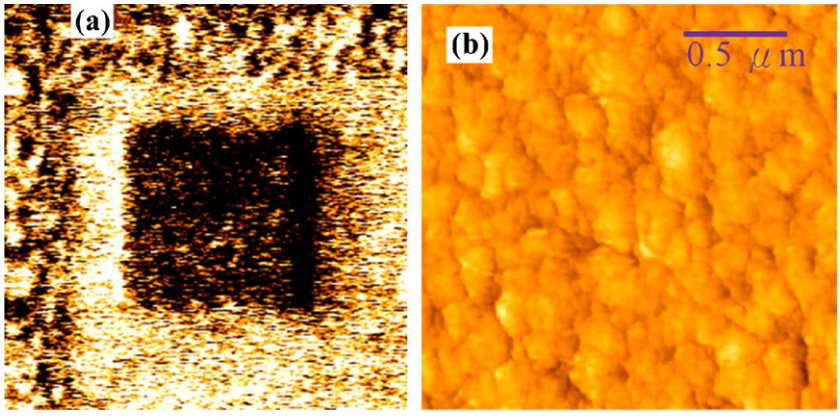

Fig. 7. (a) PFM image of in-situ film: top and right edge areas were virgin surface, large white square was poled with −10 V, and the middle dark square was switched with +10 V. (b) Surface morphology of in-situ films revealed by AFM.

stoichiometry of BFO. Because the films were grown in-situ at high temperature, it was possible to avoid the intermediate phases completely by setting accurate thermodynamic parameters and using closely matched substrates; while for the films grown by sintering, once the intermediate phases formed during heating, it was very difficult to decompose completely. The fast deposition rate (∼5 nm/min) used in this study might have helped to obtain an accurate stoichiometry of BFO, because it minimised the effect of the different desorption rate between the Bi and Fe adatoms. The films grown at slower rate indeed showed a higher level of leakage.

The *P–E* hysteresis loops of the in-situ films are showed in Fig. 6, which were measured at room temperature with the frequency of 1.67 kHz. The loops were fully saturated and a large remanent polarisation of 64 $\mu C/cm^2$ was achieved. PFM was used to visualize the domain structures as well as the domain switching under applied fields, as shown in Fig. 7a. For comparison with the surface morphology, AFM image was also shown in Fig. 7b. The PFM images taken from the virgin surface without any previous application of DC bias revealed very fine spontaneous domains, as those shown in the left and top edge areas of Fig. 7a. The large white square in Fig. 7a had previously been poled with −10 V DC bias, and the smaller dark square in the middle was subsequently switched with +10 V DC bias following the poling. The results showed that the films were electrically writable.

5. Conclusions

Epitaxial BFO films could be grown on the STO substrates either by post-deposition annealing at 600 °C in the flowing Ar atmosphere, or by in-situ growth during sputtering at 600 °C and 2 mTorr pO_2. Although the sintered films grown on the STO substrates had a right Bi/Fe stoichiometry and were epitaxial with a better texture than the in-situ films, they showed much larger leakage currents, presumably due to the residual traces of intermediate phases formed during heating. Therefore, there were at least two material issues to be solved before good ferroelectric properties could be achieved: one was the impurity phases in the films and the other was the nonstoichiometry in the pure BFO phase. Under the right growth parameters, the in-situ films grown on the LNO buffered $SrTiO_3$ showed fully saturated *P–E* hysteresis loops with large remanent polarisation of 64 $\mu C/cm^2$ at room temperature. PFM was used to examine the ferroelectric domain structures of the films. When scanned without DC bias, fine spontaneous domains were observed. Under ±10 V DC bias, PFM confirmed that the domains could be poled and switched.

Acknowledgments

This work was supported by the National Science Council under the grant number: NSC-96-2628-E-006-010-MY3, and by the National Cheng Kung University via the Landmark Projects.

References

1. Spaldin, N. A. and Fiebig, M., The renaissance of magnetoelectric multiferroics. *Science*, 2005, **309**, 391–392.
2. Ramesh, R. and Spaldin, N. A., Multiferroics: progress and prospects in thin films. *Nat. Mater.*, 2007, **6**, 21–29.
3. Cheong, S. W. and Mostovoy, M., Multiferroics: a magnetic twist for ferroelectricity. *Nat. Mater.*, 2007, **6**, 13–20.
4. Scott, J. F., Multiferroic memories. *Nat. Mater.*, 2007, **6**, 256–257.
5. Murashav, V. A., Rakov, D. N., Ionov, V. M., Dubenko, I. S., Titov, Y. U. and Gorelik, V. S., Magnetoelectric (Bi, Ln)FeO_3 compounds: crystal growth, structure and properties. *Ferroelectrics*, 1994, **162**, 11–21.
6. Popov, Yu. F., Kadomtseva, A. M., Vorobev, G. P. and Zvezdin, A. K., Discovery of the linear magnetoelectric effect in magnetic ferroelectric $BiFeO_3$ in a strong magnetic field. *Ferroelectrics*, 1994, **162**, 135–140.
7. Teague, R., Gerson, R. and James, W. J., Dielectric hysteresis in single crystal $BiFeO_3$. *Solid State Commun.*, 1970, **8**, 1073–1078.
8. Wang, J., Neaton, J. B., Zheng, H., Nagarajan, V., Ogale, S. B., Liu, B. *et al.*, Epitaxial $BiFeO_3$ multiferroic thin film heterostructures. *Science*, 2003, **299**, 1719–1722.
9. Lebeugle, D., Colson, D., Forget, A. and Viret, M., Very large spontaneous electric polarization in $BiFeO_3$ single crystals at room temperature and its evolution under cycling fields. *Appl. Phys. Lett.*, 2007, **91**, 022907.
10. Powder Diffraction File™ (PDF) #46-0416, The International Centre for Diffraction Data® (ICDD).
11. PDF #20-0836, ICDD.
12. PDF #33-0710, ICDD.
13. PDF #26-1136, ICDD.
14. PDF #43-0184, ICDD.
15. Bea, H., Bibes, M., Barthelemy, A., Bouzehouane, K., Jacquet, E., Khodan, A. *et al.*, Influence of parasitic phases on the properties of $BiFeO_3$ epitaxial thin films. *Appl. Phys. Lett.*, 2005, **87**, 072508.
16. Qi, X., Wei, M., Lin, Y., Jia, Q. X., Zhi, D., Dho, J. *et al.*, High-resolution X-ray diffraction and transmission electron microscopy of multiferroic $BiFeO_3$ films. *Appl. Phys. Lett.*, 2005, **86**, 071913.
17. Wang, Y. P., Zhou, L., Zhang, M. F., Chen, X. Y., Liu, J. M. and Liu, Z. G., Room-temperature saturated ferroelectric polarization in $BiFeO_3$ ceramics synthesized by rapid liquid phase sintering. *Appl. Phys. Lett.*, 2004, **84**, 1731–1733.
18. Qi, X., Dho, J., Tomov, R., Blamire, M. G. and MacManus-Driscoll, J. L., Greatly reduced leakage current and conduction mechanism in aliovalent-ion-doped $BiFeO_3$. *Appl. Phys. Lett.*, 2005, **86**, 062903.
19. Gmelins Handbuch der anorganischen Chemie, System-Nummer 19, Wismut und Radioaktive Isotope, 8 vollig neu bearbeitete Aufl, Verlag Chemie GmbH, Weinheim/Bergster; 1964. p. 631.
20. Inaba, H. and Matsui, T., Vaporization and diffusion of manganese-zinc ferrite. *J. Solid State Chem.*, 1996, **121**, 143–148.